Dysregulation of the MMP/TIMP Proteolytic System in Subependymal Giant Cell Astrocytomas in Patients With Tuberous Sclerosis Complex: Modulation of MMP by MicroRNA-320d In Vitro

Bongaarts, A.; de Jong, J.M.; Broekaart, D.W.M.; van Scheppingen, J.; Anink, J.J.; Mijnsbergen, C.; Jansen, F.E.; Spliet, W.G.M.; den Dunnen, W.F.A.; Gruber, V.E.; Scholl, T.; Hainfellner, J.A.; Feucht, M.; Borkowska, J.; Kotulska, K.; Jozwiak, S.; Grajkowska, W.; Buccoliero, A.M.; Caporalini, C.; Giordano, F.; Genitori, L.; Scicluna, B.P.; Schouten-van Meeteren, A.Y.N.; van Vliet, E.A.; Mühlebner, A.; Mills, J.D.; Aronica, E.

DOI
10.1093/jnen/nlaa040

Publication date
2020

Document Version
Final published version

Published in
Journal of Neuropathology and Experimental Neurology

License
CC BY-NC

J Neuropathol Exp Neurol
Vol. 79, No. 7, July 2020, pp. 777–790
doi: 10.1093/jnen/nlaa040

ORIGINAL ARTICLE

Dysregulation of the MMP/TIMP Proteolytic System in Subependymal Giant Cell Astrocytomas in Patients With Tuberous Sclerosis Complex: Modulation of MMP by MicroRNA-320d In Vitro

Anika Bongaarts, MSc, Jody M. de Jong, MSc, Diede W.M. Broekaart, MSc, Jackelien van Scheppingen, PhD, Jasper J. Anink, BSc, Caroline Mijnsbergen, BSc, Floor E. Jansen, MD, PhD, Wim G.M. Spliet, MD, Wilfred F.A. den Dunnen, MD, PhD, Victoria E. Gruber, MSc, Theresa Scholl, PhD, Johannes A. Hainfellner, MD, PhD, Martha Feucht, MD, PhD, Julita Borkowska, MD, Katarzyna Kotulska, MD, PhD, Sergiusz Jozwiak, MD, PhD, Wieslawa Grajkowska, MD, PhD, Anna Maria Buccoliero, MD, PhD, Chiara Caporalini, MD, Flavio Giordano, MD, Lorenzo Genitori, MD, Brendon P. Scicluna, PhD, Antoinette Y.N. Schouten-van Meeteren, MD, PhD, Erwin A. van Vliet, PhD, Angelika Mühlebner, MD, PhD, James D. Mills, PhD, and Eleonora Aronica, MD, PhD

Abstract

Tuberous sclerosis complex (TSC), a rare genetic disorder caused by a mutation in the *TSC1* or *TSC2* gene, is characterized by the growth of hamartomas in several organs. This includes the growth of low-grade brain tumors, known as subependymal giant cell astrocytomas (SEGA). Previous studies have shown differential expression of genes related to the extracellular matrix in SEGA. Matrix metalloproteinases (MMPs), and their tissue inhibitors (TIMPs) are responsible for remodeling the extracellular matrix and are associated with tumorigenesis. This study aimed to investigate the MMP/TIMP proteolytic system in SEGA and the regulation of MMPs by microRNAs, which are important post-transcriptional regulators of gene expression. We investigated the expression of MMPs and TIMPs using previously produced RNA-Sequencing data, real-time quantitative PCR and immunohistochemistry in TSC-SEGA samples and controls. We found altered expression of several MMPs and TIMPs in SEGA compared to controls. We identified the lowly expressed miR-320d in SEGA as a potential regulator of *MMPs*, which can decrease *MMP2* expression in human fetal astrocyte cultures. This study provides evidence of a dysregulated MMP/TIMP proteolytic system in SEGA of which *MMP2* could be rescued by microRNA-

From the Department of (Neuro)Pathology, Amsterdam UMC, University of Amsterdam, Amsterdam Neuroscience, Amsterdam, The Netherlands (AB, JMdJ, DWMB, JvS, JJA, CM, EAvV, AM, JDM, EA); Department of Pediatric Neurology, University Medical Center Utrecht Brain Center, Utrecht, The Netherlands (FEJ); Department of Pathology, University Medical Center Utrecht, Utrecht, The Netherlands (WGMS); Department of Pathology and Medical Biology, University Medical Center Groningen, University of Groningen, Groningen, The Netherlands (WFAdD); Department of Pediatrics, Medical University of Vienna, Vienna, Austria (VEG, TS, MF); Institute of Neurology, Medical University of Vienna, Vienna, Austria (JAH); Department of Neurology and Epileptology, Children's Memorial Health Institute, Warsaw, Poland (JB, KK, SJ); Department of Child Neurology, Medical University of Warsaw, Warsaw, Poland (SJ); Department of Pathology, Children's Memorial Health Institute, Warsaw, Poland (WG); Pathology Unit, Anna Meyer Children's Hospital, Florence, Italy (AMB, CC); Department of Neurosurgery, Anna Meyer Children's Hospital, Florence, Italy (FG, LG); Department of Clinical Epidemiology, Biostatistics & Bioinformatics, Center for Experimental & Molecular Medicine, Amsterdam UMC, University of Amsterdam, Amsterdam (BPS); Princess Máxima Center for Pediatric Oncology, Utrecht, The Netherlands (AYNS-vM); Department of Pediatric Oncology, Emma Children's Hospital, Amsterdam UMC, Amsterdam, The Netherlands (AYNS-vM); Swammerdam Institute for Life Sciences, Center for Neuroscience, University of Amsterdam, Amsterdam, The Netherlands (EAvV); and Stichting Epilepsie Instellingen Nederland (SEIN), Heemstede, The Netherlands (EA).

Send correspondence to: Eleonora Aronica, MD, PhD, Department of (Neuro)Pathology, Location Academic Medical Center, Amsterdam UMC, University of Amsterdam, Meibergdreef 9, 1105 AZ Amsterdam, The Netherlands; E-mail: e.aronica@amsterdamumc.nl

Anika Bongaarts, Jody M. de Jong, and Diede W.M. Broekaart contributed equally to this work.

James D. Mills and Eleonora Aronica shared senior authorship.

Supplementary Data can be found at academic.oup.com/jnen.

The research leading to these results has received funding from KIKA (Stichting Kinderen Kankervrij; A.B., A.M., A.S., B.S., E.A.); Stichting AMC Foundation (E.A.); Stichting TSC Fonds (E.A.); the Austrian Science Fund (FWF, No. J3499; A.M.); the European Union's Seventh Framework Programme (FP7/2007–2013) under Grant Agreement No. 602102 (EPITARGET; E.V., E.A.), Grant Agreement No. 602391(EPISTOP; J.S., F.J., T.S., M.F., S.J., A.M., E.A.); the European Union's Horizon 2020 Research and Innovation Programme under the Marie Sklodowska-Curie Grant Agreement No. 642881 (ECMED; E.A.); the Dutch Epilepsy Foundation, project 16-05 (D.B., E.V.); the Austrian Epilepsy Society (V.E.G.); the Polish Ministerial funds for science (years 2013–2018) for the implementation of international cofinanced project (K.K., S.J.); and internal research project of the Children's Memorial Health Institute No. S132/2013 (K.K., S.J.).

The authors have no duality or conflicts of interest to declare.

320d. Therefore, further elucidating microRNA-mediated MMP regulation may provide insights into SEGA pathogenesis and identify novel therapeutic targets.

Key Words: Extracellular matrix, Matrix metalloproteinases, MicroRNA, Subependymal giant cell astrocytoma (SEGA), Tuberous sclerosis complex.

INTRODUCTION

Tuberous sclerosis complex (TSC) is an autosomal dominantly inherited neurocutaneous disorder affecting approximately 1 million individuals worldwide (1,2). It is caused by inactivating mutations in either the *TSC1* or the *TSC2* gene (3,4) resulting in constitutive activation of the mammalian target of rapamycin (mTOR) pathway which can affect cell growth and proliferation (5–8). Several brain abnormalities are observed in patients with TSC, including cortical tubers, subependymal nodules and subependymal giant cell astrocytomas (SEGA) (9–11). SEGA are progressive low-grade tumors that develop in the first 2 decades of life in children and adolescents with TSC with a prevalence ranging from 5% to 25% (12–16). They are slow-growing tumors located near the foramen of Monro and extended growth can lead to the obstruction of the cerebrospinal fluid flow and acute hydrocephalus (16,17). Symptoms associated with growing SEGA include headaches, photophobia, diplopia, ataxia, or changes in seizure severity (18). SEGA are believed to develop from subependymal nodules and are characterized by distinctive cytomegalic cells, which display an immature neuroglial phenotype (19–22).

Genetically, there is evidence of second-hit inactivation of *TSC1* or *TSC2* in SEGA. However, in ~20% of SEGA these second-hit mutations are not observed, suggesting that additional molecular processes might be involved in SEGA growth (6,23,24). Several studies have performed transcriptional profiling of SEGA identifying differential expression of genes related to the immune system, MAPK family signaling cascades and extracellular matrix (ECM) organization (24–26). Dysregulation of ECM organization has also been seen in TSC cortical tubers with a specific role for matrix metalloproteinases (MMPs) and their endogenous inhibitors (TIMPs), suggesting that the ECM might play an important role in TSC (27–29). MMPs are calcium-dependent zinc-containing endopeptidases that are expressed with a propeptide that needs to be removed for activation (30). TIMPs are "wedge-like"-shaped molecules with 4 residues at N-terminal that form a ridge that can noncovalently bind to the active site of MMPs and thereby inactivate them (31). The MMP/TIMP proteolytic system is known to be involved in the degradation of ECM (32), tissue morphogenesis (33), cell migration (34), angiogenesis (35), blood-brain barrier (BBB) dysfunction (36), wound healing and inflammation (37). Differential expression of MMPs is found in many pathologies including cancer, where they affect proliferation and the metastasis of tumor cells (38–40).

Several MMP inhibitors exist that can regulate MMP overactivity. However, the currently available MMP inhibitors can have a variety of side effects indicating the complexity of MMP regulation (41). MicroRNAs (miRNAs) are short non-coding RNAs which are 20–25 nucleotides long and are able to regulate the expression of protein-coding genes, including *MMPs* (42,43). They are involved in many physiological processes, such as differentiation, proliferation, and development (44) and have been implicated in neurological disorders (45,46). Previous research showed several miRNAs to be differentially expressed in TSC cortical tubers and SEGA (26,28,29,47,48). In particular, miRNAs have been shown to participate in MMP regulation at the post-transcriptional level in TSC tuber-derived astroglial cultures and glioma cell lines (28,49,50).

In our previous SEGA transcriptome study, we identified differential expression of genes related to several pathways including ECM organization, but did not further study the role of the ECM in SEGA in detail (26). As MMPs and TIMPs may contribute to TSC pathology and cancer, understanding their role in SEGA development could provide new insights into the SEGA biological behavior and potential new therapeutic targets. Therefore, in this study we investigated the expression of MMPs and TIMPs in SEGA. Furthermore, we identified differentially expressed miRNAs in SEGA compared to control tissue that could regulate the expression of MMPs and further investigated the role of these miRNAs in SEGA and their regulation of MMP expression in vitro.

MATERIALS AND METHODS

Subjects

A total of 24 SEGA specimens (male/female: 16/8; age ranging from 1 to 28 years; ethnicity: Caucasian) were collected from the following hospitals: University Medical Centers Amsterdam (location Academic Medical Center, Amsterdam, the Netherlands), the University Medical Center Utrecht (Utrecht, the Netherlands), University Medical Center Groningen (Groningen, the Netherlands), Medical University of Vienna (Vienna, Austria), Children's Memorial Health Institute (Warsaw, Poland), Anna Meyer Children's Hospital (Florence, Italy) (Table 1). Twenty-two of the 24 SEGA samples included in this study were obtained from patients who met the clinical diagnostic criteria for TSC, whereas 2 samples were obtained from patients with no other clinical signs of TSC. Histological diagnosis was confirmed following the current WHO classification guidelines (51) by 2 independent neuropathologists. Additional *TSC1/TSC2* mutation analysis was performed as part of routine clinical care on blood or tumor sample DNA or was determined using massively parallel sequencing as described previously (23,52), if available (Table 1). Periventricular brain tissue along the lateral ventricle at the level of either the caudothalamic groove or hippocampus plus its associated cortex was obtained from autopsies of patients (postmortem delay less than 24 hours) who did not have TSC, epilepsy or brain tumors and served as control tissue (frozen: n = 8, male/female: 6/2; age ranging from 3 to 87 years; paraffin: n = 4, male/female: 1/3; age ranging from 2 months to 44 years). Specimens were obtained and used in accordance with the Declaration of Helsinki and this study

TABLE 1. Summary of Clinicopathological Features of Patients With SEGA

SEGA No.	Age (Years)	Gender	Mutation	Location of Tumor	Epilepsy	Age of Epilepsy Onset	Seizure Frequency	AED*	Tumor Size (mm)	Tumor Recurrence/ Regrowth	mTOR Inhibitors	Other Clinical Manifestations
1[a]	10	Male	*TSC2*	Lateral ventricle	Yes	3 years	Daily	Yes	42	No	No	Unknown
2[a]	11	Female	*TSC2*	Lateral ventricle	No	NA	NA	NA	Unknown	No	No	No other signs for TSC
3[a,b,c]	8	Male	*TSC2*	Lateral ventricle	Yes	4 months	None	Yes	31	No	No	Cortical tuber, AML
4[a]	13	Female	*TSC1*	Lateral ventricle	Yes	17 months	Monthly	Yes	40	No	No	Cortical tuber
5[a]	1	Male	*TSC2*	Lateral ventricle	Yes	1 month	Daily	Yes	30	No	Yes (nonresponder)	Multiple SEGAs, cortical tubers, drug resistant epilepsy
6[a,b]	13	Male	*TSC2*	Caudate nucleus	Yes	6 months	Weekly	Yes	20	No	Yes (responder)	Tubers, minor psychomotor delay, SEN
7[a]	14	Male	*TSC2*	Lateral ventricle	No	NA	NA	NA	5	No	No	Renal cysts
8[a]	4	Male	*TSC1*	Lateral ventricle	Yes	3 months	Monthly	Yes	5	Yes	No	Cortical tuber
9[a,b]	7	Female	*TSC2*	Lateral ventricle	Yes	5 months	Daily	Yes	45	No	No	Unknown
10[a,b,c]	17	Female	*TSC2*	Lateral ventricle	No	NA	NA	NA	27	No	No	No other signs for TSC
11[a]	1	Female	*TSC2*	Lateral ventricle	Yes	1 month	Daily	Yes	30	No	No	Cortical tuber
12[a,b,c]	13	Male	*TSC2*	Lateral ventricle	Yes	4 months	Weekly	Yes	20	Yes	No	Cortical tuber
13[a,b]	24	Male	*TSC1*	Lateral ventricle	Yes	6 years	Daily	Yes	40	No	No	Unknown
14[a,b]	8	Male	NMI	Caudate nucleus	Yes	1 year	Weekly	Yes	30	No	No	Minor psychomotor delay
15[a]	9	Male	*TSC1*	Caudate nucleus	Yes	2 years	Monthly	Yes	30	No	No	None
16[a]	28	Female	*TSC2*	Unknown	Yes	Unknown	Unknown	NA	Unknown	Unknown	No	Cortical tuber
17[a,b,d]	33	Male	*TSC2*	Basal nuclei	Yes	6 months	Daily	Yes	30	Yes	No	Cortical tubers, autism, drug resistant epilepsy, behavior problems (aggressivity)
18[a,b]	1	Male	*TSC2*	Caudate nucleus	Yes	8 months	Monthly	Yes	20	No	No	Minor psychomotor delay, cortical tubers
19[a,b]	28	Male	*TSC2*	Lateral ventricle	Yes	7 years	Daily	Yes	34	Yes	No	Unknown
20[b,c]	1	Female	*TSC2*	Lateral ventricle	No	NA	NA	NA	20	No	No	Cortical tuber
21[b,c,d]	4	Male	*TSC2*	Lateral ventricle	Yes	3 months	Daily	Yes	18	No	No	Cortical tuber, AML, autism
22[c,d]	16	Male	*TSC1*	Lateral ventricle	No	NA	NA	NA	37	No	No	SEN
23[c]	10	Male	*TSC2*	3th ventricle	Yes	3 months	Seizure free	Yes	60	No	No	Cortical tuber, AML, autism
24[c]	5	Female	*TSC2*	Lateral ventricle	Yes	1 month	Daily	Yes	66	No	No	Cortical tuber, AML, autism, FCD

SEGA samples used for RNA-Sequencing (a), RT-qPCR (b), in situ hybridization (c), and immunohistochemistry (d).

*The most commonly used AEDs are carbamazepine, vigabatrin, valproate, and topiramate, however each patient had a personalized drug treatment regime.

AED, antiepileptic drugs; AML, angiomyolipoma; FCD, focal cortical dysplasia; NA, not applicable; NMI, no mutation identified; SEGA, subependymal giant cell astrocytomas; SEN, subependymal nodule; TSC, tuberous sclerosis complex.

TABLE 2. Primer List

Gene	Forward (5′->3′)	Reverse (5′->3′)
MMP2	ATAACCTGGATGCCGTCGT	AGGCACCCTTGAAGAAGTAGC
MMP11	TCCTGAGGTCAGGTCTTGGT	CAGATTTCCAGGATTGTCAGC
MMP14	GCCTTGGACTGTCAGGAATG	AGGGGTCACTGGAATGCTC
MMP15	CAGGCCCATCAGTGTCTGG	TGGTGCCCTTGTAGAAGTAGG
MMP16	AGGGCATCCAGAAGATATATGG	GGCACTGTCGGTAGAGGTCTT
MMP17	AAGAGGAACCTGTCGTGGAG	CACCTCGTGGAAGTTCAGG
MMP19	ATGCCAGACCCTTGCAGTAG	CCCCCTTGAAAGCATAGGTC
MMP25	TCCTGGGTGGTGGAATCA	GCAACGGAAAAGGTTAACAGC
TIMP1	GGGCTTCACCAAGACCTACA	TGCAGGGGATGGATAAACAG
TIMP2	TGCAGATGTAGTGATCAGGGC	TCTCAGGCCCTTTGAACATC
TIMP3	GCTGGAGGTCAACAAGTACCA	CACAGCCCCGTGTACATCT
TIMP4	TTGGTGCAGAGGGAAAGTCT	GGTACTGTGTAGCAGGTGGTGA
EF1α	ATCCACCTTTGGGTCGCTTT	CCGCAACTGTCTGTCTCATATCAC
GAPDH	AGGCAACTAGGATGGTGTGG	TTGATTTTGGAGGGATCTCG

was approved by the Medical Ethics Committee of each institution.

RNA-Sequencing

RNA-Sequencing (RNA-Seq) data sets produced by our laboratory, were retrieved from the European Genome-phenome Archive (EGA), which is hosted by the EBI and the CRG (accession number: EGAS00001003787) (26). Data were retrieved for 19 SEGA samples and 8 control and processed as previously described (26). Briefly, sequence reads were trimmed and filtered using FastQC v0.11.5 (Babraham Institute, Babraham, Cambridgeshire, UK) and Trimmomatic v0.36. Paired-end reads were aligned to the human reference genome (GRCh38) with TopHat2 v2.0.13 and default settings (53). For the small RNA-Seq data set no mismatches were allowed between the trimmed reads and the reference genome and small RNA reads were allowed to align a maximum of 10 times. Next, the number of reads that mapped to each gene, based on Gencode v25, was determined using featureCounts from the SubRead package (54). The count matrix was normalized using the R package DESeq2 (55). Genes and small RNAs with a Benjamini-Hochberg adjusted p value < 0.05 were considered differentially expressed. Differentially expressed genes (DEGs) related to the ECM organization were identified by overlapping the ECM organization genelist from the Reactome database with the DEGs produced from the RNA-Seq data (56,57).

To identify miRNAs that could potentially target all 5 *MMP* genes with a higher expression in SEGA compared to control (*MMP2*, *MMP11*, *MMP14*, *MMP15*, and *MMP19*), miRNAs that had lower expression in SEGA (adjusted p value $<$ 0.05) as compared to control and whose expression patterns where inversely correlated with *MMP* expression were selected. The list of predicted miRNA targets for each of the differentially expressed miRNAs was retrieved from miRWalk2 (58,59). miRNAs that were predicted to target all 5 MMPs (*MMP2*, *MMP11*, *MMP14*, *MMP15*, and *MMP19*), were considered potential regulators of MMP expression.

RNA Isolation and Real-Time Quantitative PCR Analysis

For RNA isolation, cell culture or fresh brain material (12 SEGA samples and 8 control samples) was homogenized in Qiazol Lysis Reagent (Qiagen Benelux, Venlo, The Netherlands). RNA was isolated using the miRNeasy Mini kit (Qiagen Benelux, Venlo, The Netherlands) according to manufacturer's instructions. The concentration and purity of RNA were determined at 260/280 nm using a Nanodrop spectrophotometer (Thermo Fisher Scientific, Wilmington, DE). mRNA and miRNA expression was evaluated as described previously (60). Briefly, 250 ng of RNA were reverse-transcribed into cDNA using oligo dT primers. Real-time quantitative PCRs (RT-qPCR) were run according to the manufacturer's guidelines, on a Roche Lightcycler 480 thermocycler (Roche Applied Science, Basel, Switzerland) using LightCycler 480 SYBR Green I Master (Roche Applied Science, Indianapolis, IN) with the following cycling conditions: initial denaturation at 95°C for 5 minutes, followed by 50 cycles of denaturation at 95°C for 10 seconds, 65°C for 10 seconds, and 72°C for 15 seconds, annealing at 95°C for 5 seconds followed by extension on 65°C for 1 minute. PCR primers were designed using Universal Probe library (ProbeFinder version 2.53 for human, Roche Applied Science) (Table 2). Expression of miRNAs was analyzed using TaqMan microRNA assays (Applied Biosystems, Foster City, CA). cDNA was generated from 50 ng of RNA using TaqMan MicroRNA reverse transcription kit (Applied Biosystems). RT-qPCR was performed on a Lightcycler 480 Real-Time PCR System (Roche Applied Science). Quantification of the data was done using the LinRegPCR program in which linear regression on the Log(fluorescence) per cycle number data is applied to determine the amplification efficiency per sample (61). The expression of each specific product was divided by the geometric mean of the concentration of 2 reference genes (mRNA: Elongation factor 1-alpha [*EF1α*] and glyceraldehyde-3-phosphate dehydrogenase [*GAPDH*];

miRNA: the U6B small nuclear RNA gene [RNU6B] and RNU44).

Immunohistochemistry

Sections were deparaffinated in xylene (3x) and rinsed in ethanol (100%, 95%, and 70%). Antigen retrieval was performed by incubating the sections in 0.1 M sodium citrate buffer pH 6.0 at 121°C for 10 minutes using a pressure cooker. Sections were washed with phosphate buffered saline ([PBS], pH 7.4) after which they were blocked with 10% normal goat serum (NGS) for 30 minutes at room temperature. After removal of NGS, primary antibody (1:200 rabbit polyclonal IgG anti-MMP2, Abcam, Cambridge, UK; 1:500 mouse monoclonal IgG 3/κ anti-MMP14, Merck, Darmstadt, Germany) in Normal Antibody Diluent (Immunological, Duiven, The Netherlands) was added to the sections and incubated overnight at 4°C. After incubation with primary antibodies, sections were washed in PBS and stained with a polymer-based peroxidase immunohistochemistry detection kit according to manufacturer's guidelines (PowerVision Peroxidase system, ImmunoVision, Brisbane, CA). After washing, sections were stained with 3,3′-diaminobenzidine tetrahydrochloride (50 mg diaminobenzidine [DAB], Sigma-Aldrich, Zwijndrecht, the Netherlands) and H_2O_2 in Tris-HCl (0.015% final concentration). The reaction was stopped by washing with dH_2O, the sections were then counterstained with hematoxylin and dehydrated with ethanol (70%, 95%, 100%) and xylene (3x) and coverslipped.

Stainings of MMPs were quantified by measuring the optical density (OD) of SEGA and control tissue using ImageJ. For each case, 2-3 representative photographs of periventricular white matter (wm) (n = 4) and when present nearby gray matter (gm) (n = 3) were taken (20x magnification). Three OD measurements were taken after hematoxylin-DAB color deconvolution for each respective picture. Finally, the mean OD was calculated per case.

In Situ Hybridization

Paraffin slides from SEGA and autopsy controls (Table 1) were deparaffinated in xylene (3x) and rinsed in ethanol (2x 100%, 70%) and dH_2O. Sections were pretreated using a pressure cooker in 0.1 M sodium citrate buffer, pH 6.0, at 121°C for 10 minutes. The oligonucleotide probe for miR-320d (TCCTCUCAACCCAGCTUUT) contained LNA modification, 2-o-methyl modification and digoxigenin (DIG) label (RiboTask ApS, Odense, Denmark). Sections were incubated with the probe (1:750 dilution) in hybridization mix (600 mM NaCl, 10 mM HEPES, 1 mM EDTA, 5× Denhardts, 50% formamide) for 1 hour at 56°C. Sections were washed with saline-sodium citrate (SSC) 2× for 2 minutes, SSC 0.5× for 2 minutes, and SSC 0.2× for 1 minute (in agitation). After washing with sterile PBS, sections were blocked for 15 minutes with 0.02% Tween 20 and 1% NGS. Hybridization was detected with AP labeled with anti-DIG (Roche Applied Science, Basel, Switzerland). Nitro-blue tetrazolium chloride/5-bromo-4-chloro-3′-indolyphosphate p-toluidine salt was used as chromogenic substrate for AP (1:50 diluted in NTM-T buffer [100 mM Tris, pH 9.5; 100 mM NaCl; 50 mM $MgCl_2$]; 0.05% Tween 20). Expression of miR-320d was quantified by measuring the OD of SEGA and control tissue using ImageJ. For each case, 2 and 3 representative photographs of periventricular wm (n = 9) and when present nearby gm (n = 7) were taken (20x magnification). Three OD measurements were taken for each respective picture. Finally, the mean OD was calculated per case.

Cell Culture

As SEGA are thought to originate from neuroglial precursor cells that undergo an altered/impaired development, we have chosen to use a glial cell type in a developmental state; (human fetal astrocyte-enriched cells) to study the role of miR-320d on MMP expression under basal conditions. Primary fetal astrocyte-enriched cell cultures were obtained from fetal brain tissue (n = 3, 14–19 weeks of gestation) collected from medically induced abortions as described previously (47,48), with appropriate maternal written consent for brain autopsy. Briefly, blood vessels were removed and the tissue was cut into smaller fragments. The tissue was enzymatically digested by incubating at 37°C for 30 minutes with trypsin. The enzymatic reaction was stopped by adding twice the amount of astrocyte medium (DMEM/F10, 10% FCS, 5% penicillin/streptomycin, and 5% glutamine) and the cell suspension was passed through a 70-μm cell strainer. After washing 2 times with astrocyte medium, the cells were incubated at 37°C, 5% CO_2 for 48 hours after which they were thoroughly washed with PBS. Fresh medium was added twice a week and cultures reached confluency after 2 and 3 weeks. Secondary astrocyte cultures for experimental manipulation were established by trypsinizing confluent cultures and subplating onto poly-L-lysine (PLL; 15 mg/mL, Sigma-Aldrich, St. Louis, MO)-precoated 6- and 12-well plates (Costar; 50 000 cells/well in a 12-well plate for RNA isolation and RT-qPCR).

Transfection of Cell Cultures

Cells on PLL-coated plates were transfected with mimic pre-miRNA for hsa-miR-320d (50 μM; Applied Biosystems, Carlsbad, CA) for 24 hours. Cells treated with lipofectamine without mimic were used as a control. Mimics were delivered to the cells using Lipofectamine 2000 transfection reagent (Life Technologies, Grand Island, NY) in a final concentration of 50 nM.

Statistical Analysis

Statistical analyses were performed with GraphPad Prism version 5 (GraphPad Software, La Jolla, CA) and IBM SPSS Statistics 24 (IBM Corp., Armonk, NY) using the nonparametric Mann-Whitney U test or, for multiple groups, the nonparametric Kruskal-Wallis test followed by Mann-Whitney U test. A p value < 0.05 was assumed to indicate a statistical difference. Correlations were assessed with R or IBM SPSS Statistics 24, using the Spearman's rank correlation test ($p < 0.05$ and $0.7 < r > -0.7$ was considered statistically significant).

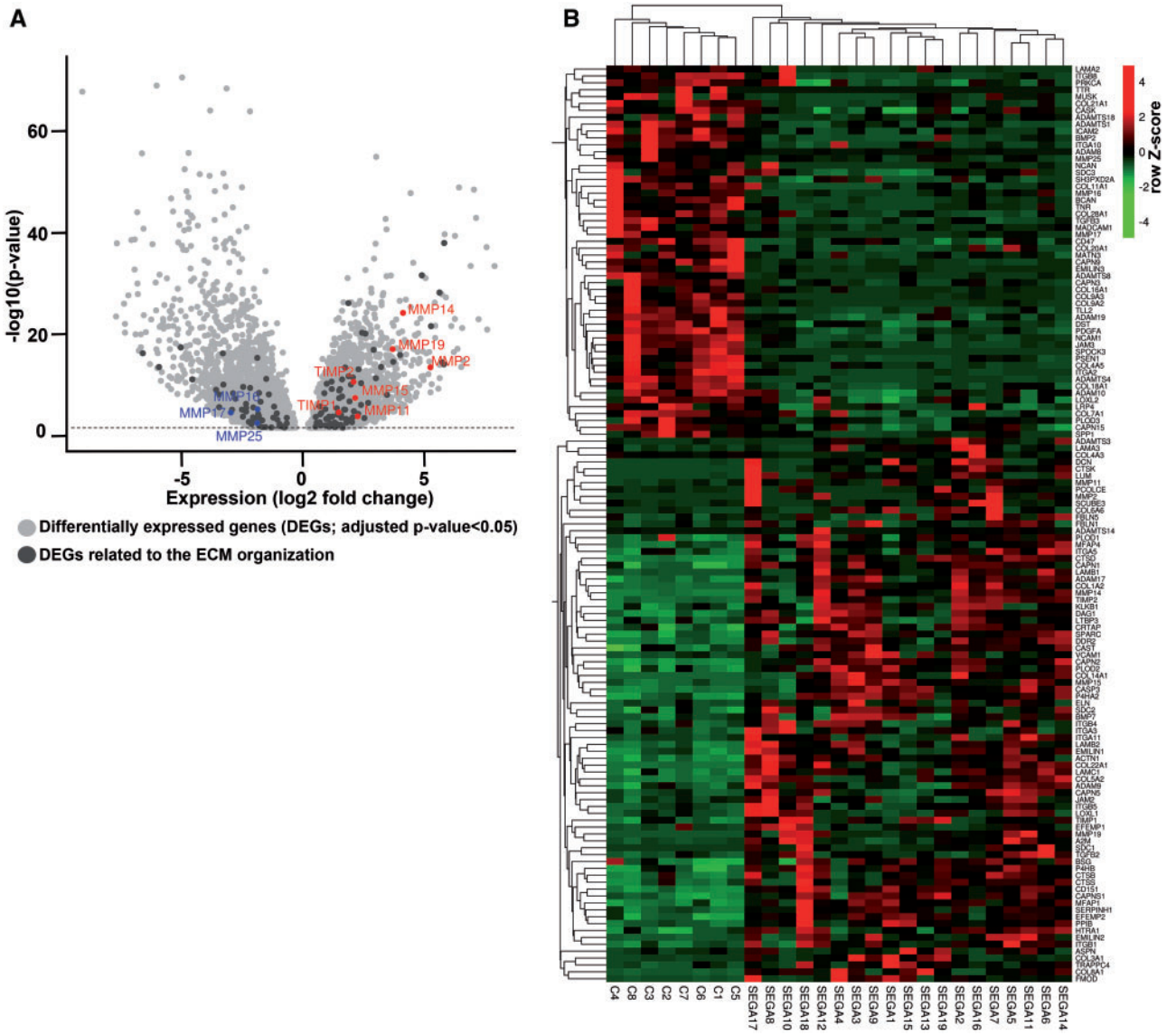

FIGURE 1. The extracellular matrix (ECM) organization in subependymal giant cell astrocytomas (SEGA). **(A)** Volcano plot showing the differentially expressed genes ([DEGs]; adjusted p value < 0.05; light gray) between SEGA and control tissue. A total of 4621 mRNAs were found to be overexpressed and 4779 underexpressed in SEGA (n = 19) as compared to control tissue (n = 8). A total of 133 DEGs were related to the Reactome-based ECM organization pathway (dark gray). Among the 133 genes *MMP2*, *MMP11*, *MMP14*, *MMP15*, *MMP19*, *TIMP1*, *TIMP2* were overexpressed and *MMP16*, *MMP17* and *MMP25* were underexpressed. **(B)** Heatmap with Z-score hierarchical clustering for the RNA expression data of DEGs related to the Reactome-based ECM organization pathway in SEGA (n = 19) and control tissue (n = 8). The color scale means the gene expression standard deviations from the mean, with green for low expression and red for the high expression.

RESULTS

MMP and *TIMP* Expression in SEGA

RNA-Seq data previously produced by our laboratory was used to specifically investigate the expression of *MMPs* and *TIMPs* in SEGA (26). In total, 19 surgical SEGA samples (obtained from 17 TSC patients and 2 patients without any clinical signs of TSC) and 8 area-matched periventricular controls (autopsy specimens) without a history of other neurological diseases were subjected to RNA-Seq (26) (Table 1). Differential gene expression analysis identified 4621 genes overexpressed and 4779 underexpressed (adjusted p value $<$ 0.05) in SEGA samples compared to control tissue, of which 133 genes belong to the Reactome-based ECM organization pathway (Fig. 1A). Furthermore, the gene expression of these 133 genes could be used to separate the control and SEGA samples (Fig. 1B). Among the 133 genes identified *MMP2*, *MMP11*, *MMP14*, *MMP15*, *MMP16*, *MMP17*, *MMP19*,

TABLE 3. Differentially Expressed MMPs and TIMPs in SEGAs as Compared to Control Tissue

mRNA	*MMP2*	*MMP11*	*MMP14*	*MMP15*	*MMP16*	*MMP17*	*MMP19*	*MMP25*	*TIMP1*	*TIMP2*	*TIMP3*	*TIMP4*
BaseMean	7918.05	37.645	10816.6	498.068	402.112	129.329	407.115	32.0523	3772.49	27817.6	7473.16	533.5
Log2 FoldChange	5.26395	2.27464	4.13891	2.16889	−1.8413	−2.9409	3.71133	−1.8555	1.49335	2.10445	1.16444	1.77748
LfcSE	0.69286	0.59681	0.40108	0.39237	0.40482	0.69567	0.4314	0.62099	0.35208	0.31444	0.39523	0.6906
Stat	7.59742	3.81131	10.3194	5.52764	−4.5484	−4.2274	8.60299	−2.9879	4.24149	6.69264	2.94624	2.57382
p Value	3E−14	0.00014	5.8E−25	3.2E−08	5.4E−06	2.4E−05	7.8E−18	0.00281	2.2E−05	2.2E−11	0.00322	0.01006
Adjusted p value	8.4E−13	0.00057	6.5E−23	3.2E−07	3.2E−05	0.00012	3.8E−16	0.00802	0.00011	4E−10	0.00901	0.02403
Control 1	182.645	0	275.352	117.612	711.21	395.731	16.6041	22.1388	599.132	8743.45	4679.59	253.213
Control 2	453.634	13.9939	2239.02	141.105	928.26	165.594	45.4801	46.6462	3266.4	6040.69	2222.69	198.246
Control 3	42.8228	0	1082.38	47.2527	218.544	160.955	57.5892	270.226	3397.76	6622.76	7322.69	243.647
Control 4	224.35	0	213.81	213.81	2567.23	1075.08	30.1142	76.7911	1017.86	4381.61	3014.43	367.393
Control 5	252.687	19.151	588.894	120.758	808.067	170.231	32.9823	26.0667	691.565	6271.96	3574.86	165.976
Control 6	61.4008	20.4669	467.816	273.38	381.562	251.451	48.2435	58.4769	2150.49	12322.6	4942.76	0
Control 7	96.9527	9.61515	1185.87	118.587	497.584	83.3313	18.429	26.4416	1578.49	10136	4299.57	92.9464
Control 8	26.5541	6.88439	70.8108	63.9265	541.9	518.296	57.0421	21.6366	215.383	10492.8	1072	33.4385
SEGA1	350.288	99.906	10408.7	1214.91	83.8717	3.70022	145.542	0	2070.89	8752.26	29806.5	477.329
SEGA2	19 637.7	35.9809	27384.9	721.305	174.845	38.2298	278.29	12.9307	1977.83	59003.1	4009.06	558.267
SEGA3	326.138	14.7288	25176.8	1391.87	131.507	0	193.579	7.36442	5079.34	36881	25576.6	26.3015
SEGA4	170.591	28.7514	12355.4	1046.55	55.586	0.95838	208.927	17.2508	2749.59	28491.6	8542.03	411.144
SEGA5	3984.96	62.718	17916.6	324.24	427.192	77.51	1091.06	21.8921	3878.46	51157.2	4553.56	186.971
SEGA6	15 097.6	29.4384	12479.7	817.734	711.974	7.63219	390.332	6.54187	3086.67	41390.4	4661.08	757.767
SEGA7	48 776.7	90.7741	20215.5	380.941	216.461	33.3614	443.785	0	3766.74	55441.3	6153.24	2215.04
SEGA8	924.957	28.444	6737.01	243.354	92.7064	189.627	31.6044	4.21393	3188.89	29829.3	6329.32	51.6206
SEGA9	1171.21	8.16435	12124.8	866.163	107.621	5.1955	235.282	27.4619	3664.31	40081.8	6475.81	565.567
SEGA10	215.259	11.5576	1533.54	18.781	85.237	4.33408	1272.78	26.0045	9095.07	6490.29	3561.89	0
SEGA11	1669.2	53.9765	14927.1	1188.5	250.533	99.8056	1758.82	42.7738	3814	39267.4	7084.16	89.6214
SEGA12	31 142.2	17.1046	30274.5	599.319	276.305	3.94722	809.18	7.23657	2407.8	68810.6	1033.51	360.513
SEGA13	5142.81	22.1056	7551.02	466.819	202.852	0	274.37	50.7129	6522.46	16450.5	10090.6	3808.67
SEGA14	7749.68	11.8189	19932.6	424.3	87.4601	11.8189	579.128	0	5109.33	45514.7	9754.17	33.093
SEGA15	444.297	56.1474	9724.48	961.829	69.5739	9.76476	281.957	4.88238	6996.45	18311.4	13725.6	86.6623
SEGA16	13 231	11.3008	16272.1	386.488	479.155	75.7155	305.122	2.26017	2356.22	48061.3	2552.86	1237.44
SEGA17	44 702.6	271.937	21 368.3	243.825	195.06	89.4982	523.794	12.0478	5108.28	57 122.2	16 237	1060.78
SEGA18	4069.25	76.7546	12 831.9	469.336	211.39	20.1324	1323.7	22.6489	9297.37	13 926.6	5554.01	54.1057
SEGA19	13 639.8	14.6952	6709.02	585.136	343.333	0	538.378	50.7652	8770.36	21 080.9	4945.6	1068.74

MMPs, matrix metalloproteinases; SEGA, subependymal giant cell astrocytomas; TIMPs, tissue-inhibitors of metalloproteinases.

MMP25, *TIMP1* and *TIMP2* were differentially expressed (Fig. 1A, B). Though not present in the ECM organization pathway, the other 2 TIMPs found in the brain, *TIMP3* and *TIMP4*, were also among the 9400 DEGs (Table 3). These MMPs and TIMPs were selected for further validation with RT-qPCR. Higher expression of *MMP2*, *MMP11*, *MMP14*, *MMP15*, *MMP19*, *TIMP1*, *TIMP2*, and *TIMP3* was found in SEGA ($n = 12$) as compared to control tissue ($n = 8$; $p < 0.05$; Fig. 2A–H). The expression of *MMP17* (Fig. 2I) was lower in SEGA as compared to control tissue, whereas *MMP16*, *MMP25*, and *TIMP4* expression did not change (Fig. 2J–L). RNA expression of *MMPs* and *TIMPs* did not correlate with the age at epilepsy onset, age at surgery, or size of the tumor ($p > 0.05$ and $-0.7 < r > 0.7$ for both RT-qPCR and RNA-Seq data). Furthermore, RNA expression of *MMPs* and *TIMPs* was not associated with the clinical features such as gender, TSC mutation, epilepsy, or preoperative seizure frequency (Mann-Whitney U test or, for multiple groups, the nonparametric Kruskal-Wallis test; $p > 0.05$ for both RT-qPCR and RNA-Seq data). *MMP19* expression based on the RT-qPCR was higher in recurrent/regrown SEGA compared to nonrecurrent/regrown SEGA (Supplementary Data Fig. S1; $p = 0.0485$). However, RNA-Seq data did not show differences between recurrent/regrown SEGA and nonrecurrent/regrown SEGA ($p = 0.96$).

MMP2 and MMP14 Protein Expression Increased in SEGA

As *MMP2* and *MMP14* had the most abundant RNA expression in SEGA compared to controls they were selected for further analysis at the protein level. To study cellular localization and distribution, and to quantify protein expression of MMP2 and MMP14 in SEGA, immunohistochemistry was performed on SEGA and periventricular control tissue slides (Fig. 3A–F). In periventricular control tissue both MMP2 and

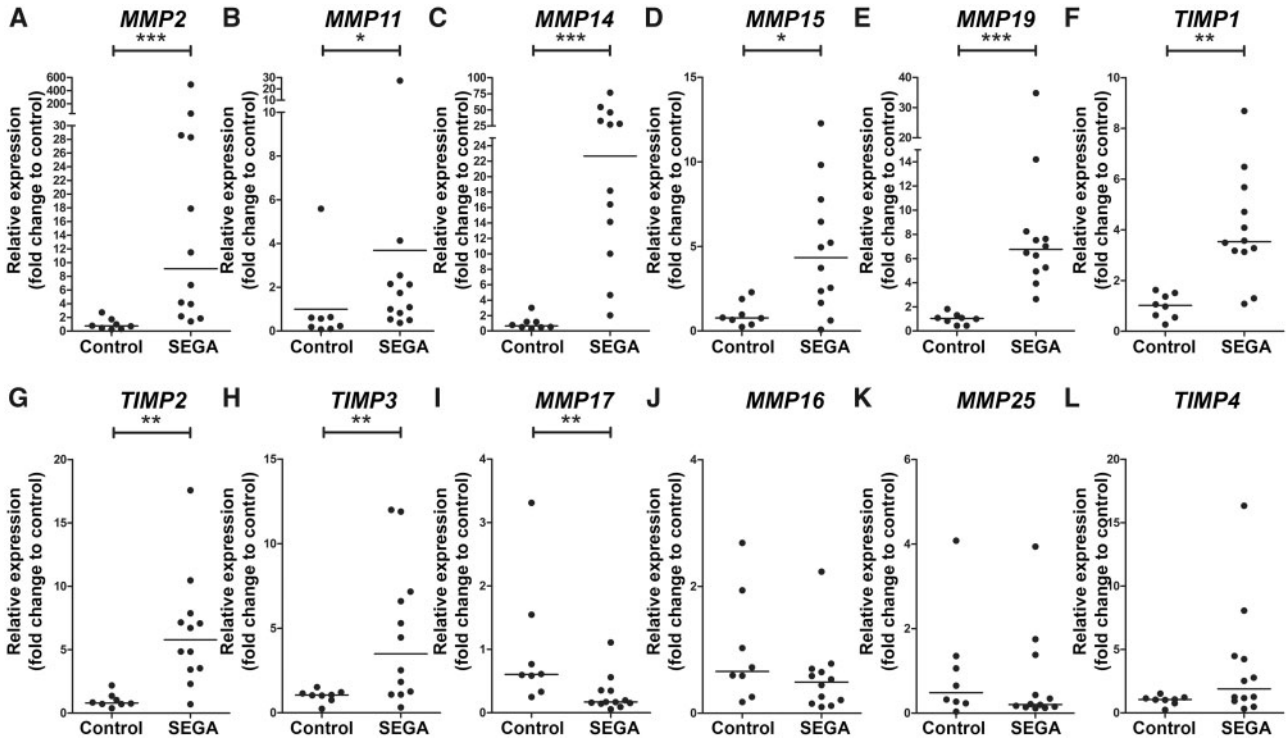

FIGURE 2. Gene expression *MMPs* and *TIMPs* differentially expression in subependymal giant cell astrocytomas (SEGA) compared to controls. **(A–L)** Gene expression was studied using RT-qPCR analysis of *MMP2* **(A)**, *MMP11* **(B)**, *MMP14* **(C)**, *MMP15* **(D)**, *MMP19* **(E)**, *TIMP1* **(F)**, *TIMP2* **(G)**, *TIMP3* **(H)**, *MMP17* **(I)**, *MMP16* **(J)**, *MMP25* **(K)**, TIMP4 **(L)** in SEGA (n = 12) and controls (n = 8). Data are expressed relative to the expression observed in control tissue. *$p < 0.05$, **$p < 0.01$, ***$p < 0.001$, Mann-Whitney U test.

MMP14 were not detected in glial cells in the wm. In nearby cortex tissue, low immunoreactivity of MMP2 and MMP14 was observed in neurons (Fig. 3A, B). In SEGA, moderate to high immunoreactivity of MMP2 and MMP14 was found in giant cells (Fig. 3C, D). The OD of MMP2 and MMP14 was higher in SEGA as compared to periventricular wm of controls (Fig. 3F; $p < 0.05$).

miR-320d as a Predictive Regulator of MMPs Is Expressed at Lower Levels in SEGA Compared to Control

To identify miRNAs that target *MMP2*, *MMP11*, *MMP14*, *MMP15*, and *MMP19*, differentially expressed miRNAs with a lower expression in SEGA as compared to controls were evaluated with miRWalk2. Based on small RNA-Seq data, we found 49 miRNAs with lower expression in SEGA as compared to controls. Six miRNAs (miR-320d, miR-320b, miR-320c, miR-625-5p, miR-330-5p, and miR-3200-3p) were predicted to target all 5 *MMPs* (*MMP2*, *MMP11*, *MMP14*, *MMP15*, and *MMP19*) with a higher expression in SEGA as compared to controls (Fig. 4A). Spearman correlations using the RNA-Seq data were calculated between each miRNA and their predicted MMP target (Table 4). miR-320d showed the strongest negative correlation with all 5 *MMPs* (*MMP2*: R: −0.484, $p = 0.010$; *MMP11*: R: −0.459, $p = 0.016$; *MMP14*: R: −0.572, $p = 0.002$; *MMP15*: R: −0.471, $p = 0.013$; *MMP19*: R: −0.433, $p = 0.024$) and was therefore selected for further analysis. Using RT-qPCR the lower expression of miR-320d in SEGA as compared to control samples was validated (Fig. 4B). To study the downregulation of miR-320d on a cellular level, in situ hybridization was performed (Fig. 4C). In control tissue, miR-320d is abundant in glial cells in periventricular wm and neuronal cells, whereas in SEGA miR-320d was not detected. The OD of miR-320d was lower in SEGA as compared to controls (Fig. 4D; $p < 0.05$).

Regulation of *MMP* by miR-320d Mimic Transfection in Fetal Astrocytes

To study regulation of *MMP2*, *MMP11*, *MMP14*, *MMP15* and *MMP19* by miR-320d, fetal astrocytes were transfected with miR-320d mimic. RT-qPCR revealed that transfection with 50 nM miR-320d mimic led to a higher expression of miR-320d (Fig. 5A; $p < 0.05$). RNA expression of *MMP2*, *MMP11*, *MMP14*, *MMP15* and *MMP19* was determined 24 hours after miR-320d transfection using RT-qPCR, and showed a lower expression of *MMP2* in miR-320d mimic transfected cells compared to control (Fig. 5B; $p = 0.002$), whereas the expression of *MMP11*, *MMP14*, *MMP15* and *MMP19* did not differ between conditions (Fig. 5C–F).

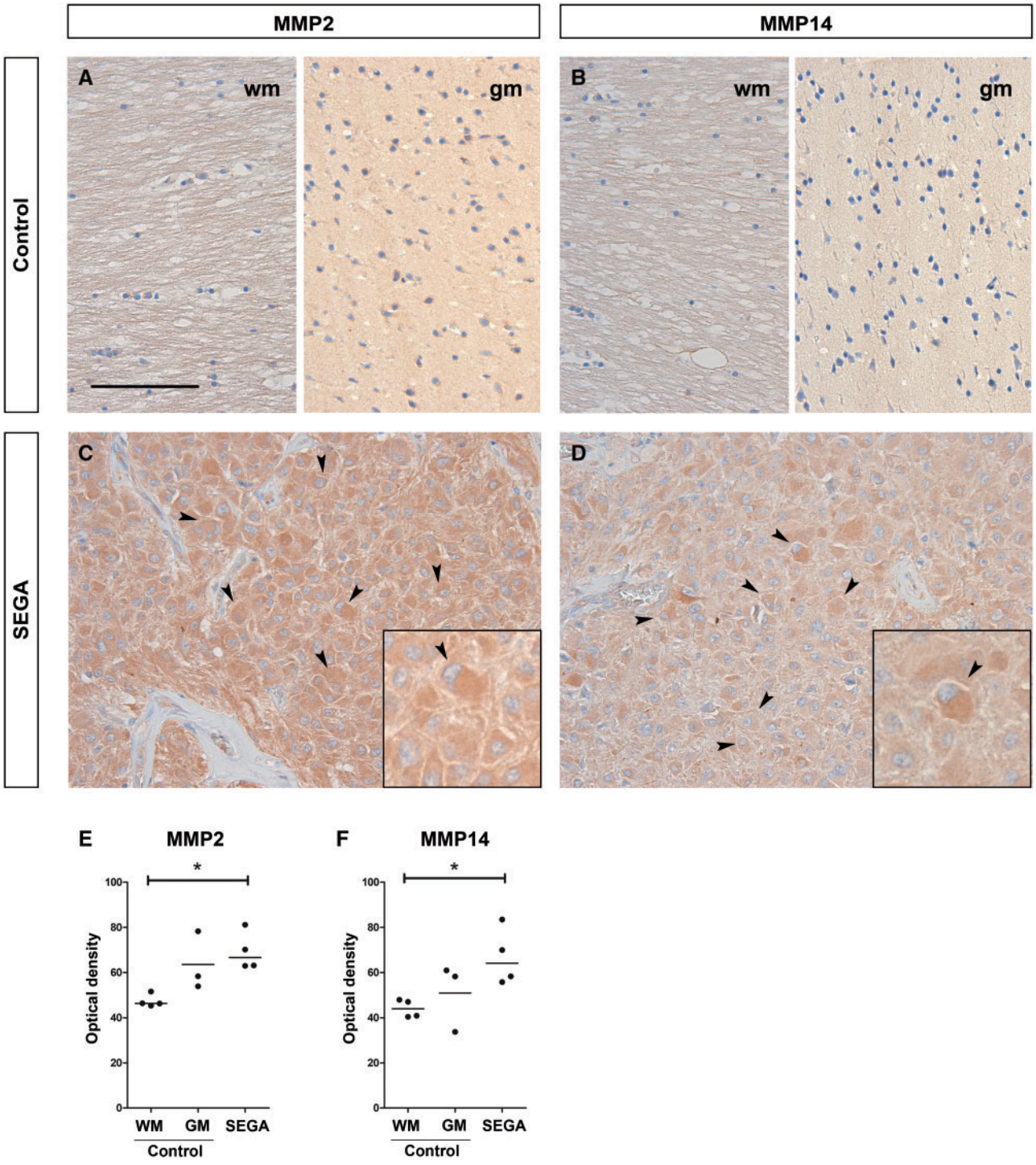

FIGURE 3. Protein expression of MMP2, MMP14 in subependymal giant cell astrocytomas (SEGA). **(A–D)** A moderate to high immunoreactivity of MMP2 **(C)** and MMP14 **(D)** was observed in SEGA, while no to low immunoreactivity was seen in periventricular white matter (wm) and gray matter (gm) control tissue, respectively **(A, B)**. Insets show a higher magnification of giant cells (indicated with arrows) in SEGA. Scale bar: 100 μm; insets: 50 μm. **(E, F)** The optical density per case for the immunoreactivity of MMP2 **(E)** and MMP14 **(F)** in periventricular control tissue (n = 3/4) and SEGA (n = 4). *$p < 0.05$, **$p < 0.01$, ***$p < 0.001$, Mann-Whitney U test.

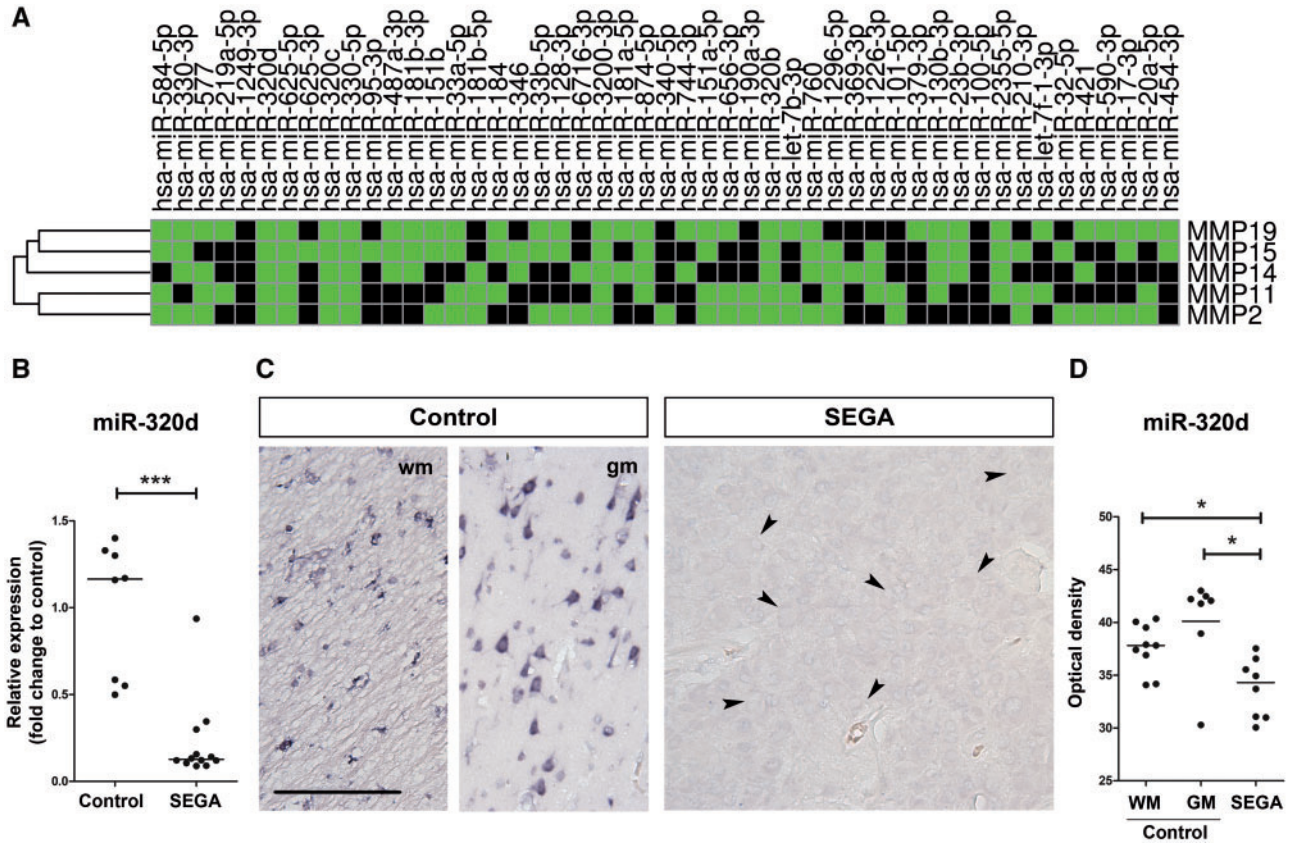

FIGURE 4. miR-320d is a predictive regulator of MMPs and is lower expressed in subependymal giant cell astrocytomas (SEGA) compared to control. **(A)** Heatmap showing all underexpressed miRNAs in SEGA as compared to controls (adjusted p value <0.05) predicted to target *MMP2*, *MMP11*, *MMP14*, *MMP15*, and/or *MMP19* (based on miRWalk2). Green boxes indicate *MMP19*, *MMP15*, *MMP14*, *MMP11*, and/or *MMP2* as predicted target of a specific miRNA. **(B)** Relative expression of miR-320d in SEGA (n = 12) as compared to control tissue (n = 8). Data are expressed relative to the expression observed in control tissue. *p < 0.05, **p < 0.01, ***p < 0.001, Mann-Whitney U test. **(C)** In situ hybridization of miR-320d in periventricular white matter (wm) and gray matter (gm) control and SEGA tissue. Giant cells are indicated with arrows. Scale bar: 100 μm. **(D)** The optical density per case for the in situ hybridization signal of miR-320d in periventricular control tissue (n = 7/9) and SEGA (n = 8). *p < 0.05, ***p < 0.001, Mann-Whitney U test.

TABLE 4. Correlations of *MMPs* and *TIMPs* With miR-320d, miR-320b, miR-320c, miR-625-5p, miR-330-5p, and miR-3200-3p

MicroRNA→ Gene↓	miR-320d (p Value; r)	miR-320b (p Value; r)	miR-320c (p Value; r)	miR-625-5p (p Value; r)	miR-330-5p (p Value; r)	miR-3200-3p (p Value; r)
MMP2	0.010; −0.484	0.028; −0.423	0.052; −0.379	0.243; −0.233	0.271; −0.22	0.493; −0.138
MMP11	0.016; −0.459	0.024; −0.432	0.012; −0.477	0.03; −0.419	0.072; −0.351	0.062; −0.363
MMP14	0.002; −0.572	0.024; −0.433	0.007; −0.503	0.019; −0.45	0.044; −0.391	0.061; −0.366
MMP15	0.013; −0.471	0.028; −0.422	0.011; −0.481	<0.001; −0.627	0.024; −0.433	<0.001; −0.644
MMP16	0.074; 0.349	0.315; 0.201	0.058; 0.37	0.021; 0.443	0.06; 0.367	0.004; 0.532
MMP17	0.040; 0.397	0.058; 0.369	0.013; 0.47	0.002; 0.56	0.093; 0.33	<0.001; 0.633
MMP19	0.024; −0.433	0.083; −0.340	0.031; −0.416	0.168; −0.273	0.269; −0.22	0.518; −0.13
MMP25	0.050; 0.380	0.125; 0.302	0.039; 0.399	0.095; 0.328	0.085; 0.337	0.202; 0.254
TIMP1	0.372; −0.179	0.634; −0.096	0.403; −0.168	0.489; −0.139	0.565; −0.116	0.477; −0.143
TIMP2	0.001; −0.590	0.014; −0.467	0.011; −0.483	0.034; −0.41	0.014; −0.466	0.084; −0.338
TIMP3	0.348; −0.188	0.475; −0.143	0.275; −0.218	0.096; −0.327	0.073; −0.351	0.014; −0.467
TIMP4	0.259; −0.225	0.102; −0.321	0.383; −0.175	0.308; −0.204	0.251; −0.229	0.099; −0.324

MMPs, matrix metalloproteinases; TIMPs, tissue-inhibitors of metalloproteinases.

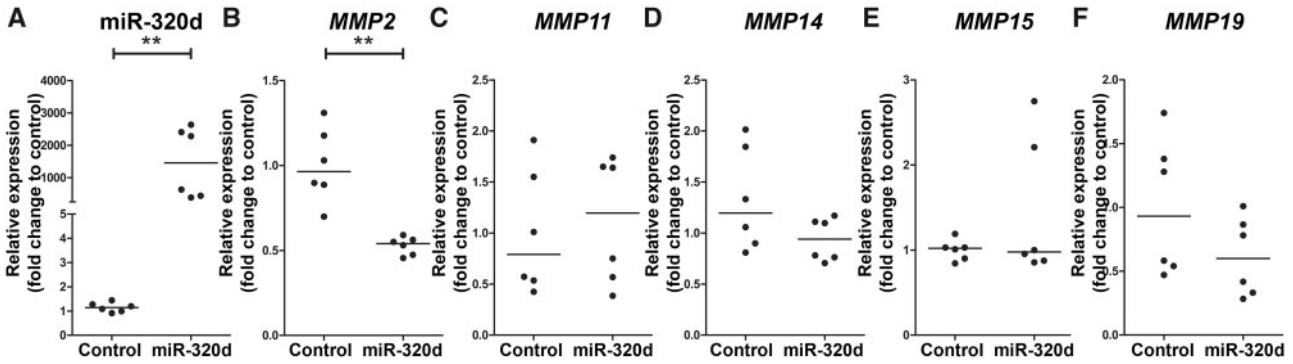

FIGURE 5. *MMP* expression after transfection with miR-320d in fetal astrocytes. (**A**–**F**) TaqMan PCR of miRNA-320d **(A)** and RT-qPCR of *MMP2* **(B)**, *MMP11* **(C)**, *MMP14* **(D)**, *MMP15* **(E)**, and *MMP19* **(F)** in fetal astrocytes transfected with miRNA-320d mimic (miR-320d) for 24 hours (n = 2 biological triplets and 3 technical duplicates). Data are normalized to lipofectamine (control). **p < 0.01, Mann-Whitney U test.

DISCUSSION

This study provides evidence that the MMP/TIMP proteolytic system is dysregulated in SEGA. We showed higher expression of *MMP2*, *MMP11*, *MMP14*, *MMP15*, *MMP19*, and their endogenous inhibitors *TIMP1*, *TIMP2* and *TIMP3* and lower expression of *MMP17* in SEGA as compared to periventricular control tissue. Furthermore, we identified the lowly expressed miR-320d in SEGA compared to controls as a potential MMP regulator that can decrease *MMP2* expression in vitro.

MMP and TIMP Expression in SEGA

Dysregulation of ECM organization in TSC cortical tubers and SEGA has been suggested by several transcriptome studies showing differential expression of genes related to the gene ontology term ECM organization, however the ECM has not been studied in detail in SEGA (24,26,27,29). In this study, we identified higher expression of *MMP2*, *MMP11*, *MMP14*, *MMP15*, *MMP16*, *MMP17*, *MMP19*, *MMP25*, *TIMP1*, *TIMP2* and *TIMP3* in SEGA as compared to controls. This suggests that the dysregulation of the MMP/TIMP proteolytic system is conserved across TSC pathology and might also affect migration during early brain development in TSC. In our previous study, we showed higher expression of MMPs and TIMPs in non-SEGA material of TSC patients. Among others, higher expression of *MMP2*, *MMP14*, *TIMP1*, *TIMP2* and *TIMP3* was observed in cortical tubers of TSC patients as compared to control cortex. Moreover, increased protein expression of MMP2 and MMP14 was also observed in tubers of TSC patients and the expression of MMPs and TIMPs was associated with neuroinflammation and BBB dysfunction (28). This indicates that the overexpression of MMPs might not be SEGA-specific, but it does underlie its relevance in the dysfunctional microenvironment that is present in TSC-related brain alterations. Multiple studies have shown the presence of neuroinflammation in TSC cortical tubers and SEGA (24,26,27,29,62–64). Previously, we have shown that the immune system is among the most represented enriched pathways in SEGA (26). Furthermore, upregulation of several cytokines, including interleukin 33, TNF Superfamily member 8, C-C Motif Chemokine Ligand 3, and C-C Motif Chemokine Ligand 5 was observed in SEGA compared to controls. Moreover, albumin extravasation, with uptake in astrocytes, has been reported in cortical tubers and SEGA of TSC patients, suggesting that alterations in BBB permeability are associated with the inflammation in TSC brain lesions (62,65). MMPs can contribute to the inflammatory response by cleaving propeptides of cytokines such as TNFα and IL-1β, thereby activating them (66–68). In turn, neuroinflammation can increase the expression and activity of MMPs and infiltrating immune cells such as leukocytes, which are a major source of MMP9 (69,70). The link between the neuroinflammation and MMPs in SEGA deserves further investigation.

MMPs are also known to be involved in cancer pathology in multiple ways, including intravasation and extravasation of tumor cells, migration of tumor cells in the brain and adhesion of metastatic cells to the ECM (38–40). Previous research has shown that higher *MMP2* expression can be a predictor for overall survival of patients with astrocytomas (71). In another study, it was found that *MMP14* and *MMP19* had higher expression in gliomas compared to healthy control tissue, and that coexpression of *MMP14* and *MMP19* predicted poor survival in human glioma (72,73). Furthermore, a correlation between higher *MMP11* and *MMP19* expression and increased WHO-grading of malignant tumors has been suggested (74). However, SEGA are slow-growing, WHO grade I tumors that are not associated with poor survival rates, suggesting that in SEGA the higher MMP expression is most likely not linked to overall survival (51). Furthermore, in this study we did not find any correlation with the clinical traits investigated, including preoperative seizure frequency, duration of epilepsy, size of the tumor, and tumor recurrence/regrowth. A previous study found increased expression of TIMP1 and TIMP2 in grade I brain tumors compared to grade II or III tumors (75). Furthermore, it has been shown that TIMP2, is also involved in the activation of pro-MMP2 together with MMP14 (76,77). We found a higher expression of MMP inhibitors *TIMP1*, *TIMP2* and *TIMP3* in SEGA as compared to control tissue. The higher expression of *TIMPs* may act as a compensatory mechanism for higher *MMP* expression, which could explain why the higher expression of *MMP2*, *MMP11*,

MMP14, *MMP15*, and *MMP19* does not lead to metastases and excessive growth in SEGA. Interestingly, we found that *MMP19* was highly expressed in recurrent/regrown SEGA as compared to nonrecurrent/regrown SEGA using RT-qPCR analysis. Previous studies found a correlation between *MMP19* expression and tumor malignance/invasion (72,74,78). Therefore, *MMP19* expression could potentially be utilized as a biomarker for recurrence/regrowth. However, our sample size of recurrent/regrown SEGA was small and this effect was not found in the RNA-Seq data, indicating that further investigation is required.

miR-320d Is a Predictive Regulator of MMPs and Is Expressed at Lower Levels in SEGA Compared to Control

Previous research has shown the importance of miRNAs in TSC and SEGA (26,29) and their role in regulating MMP expression (28,79). In this study, we identified 6 miRNAs (miR-320d, miR-320b, miR-320c, miR-625-5p, miR-330-5p, and miR-3200-3p) with lower expression in SEGA as compared to controls that could potentially target MMP expression. Research from Qin et al (49) has shown that downregulation of miR-320d in gliomas predicted lower survival rates and increased growth and proliferation. However, in our study we did not find a correlation between the expression of miR-320d and the size of tumor or tumor recurrence/regrowth. Furthermore, Qin et al (49) indicated miR-320d as a regulator of *MMP2*, decreasing MMP2 protein expression in glioma cell lines, inducing cell apoptosis and suppressing cell growth and migration. In accordance with this study, we found that miR-320d can target *MMP2* in human fetal astrocytes, but did not affect the expression of *MMP11*, *MMP14*, *MMP15*, and *MMP19*. Since the interaction of miR-320d was based on prediction tools, it could be that these MMPs are not responsive to this miRNA, however, further investigation is needed. Alternatively, it could be of interest to combine miR-320d with the other 5 miRNAs predicted to target *MMP2*, *MMP11*, *MMP14*, *MMP15* and *MMP19* (miR-320b, miR-625-5p, miR-320c, miR-330-5p, and miR-3200-3p) to increase the regulatory effect on MMP expression.

Taken together, this study provides evidence that both MMPs and TIMPs are highly expressed in SEGA compared to control tissue, indicating that the MMP/TIMP proteolytic system is dysregulated in SEGA as observed in tubers of TSC patients. The MMP-targeting miR-320d is downregulated in SEGA. In human fetal astrocytes, the dysregulation of *MMP2* can be normalized by miR-320d. We therefore conclude that targeting *MMPs* potentially with miR-320d alone or in combination with other *MMP* targeting miRNAs could be of interest as a therapeutic intervention for TSC patients with SEGA.

ACKNOWLEDGMENTS

The authors thank all supporters of the TSC brain bank (Laboratory of Molecular and Cellular Neurobiology, International Institute of Molecular and Cell Biology, Warsaw, Poland: J. Jaworski, A. Tempes; The Service d' Anatomie Pathologique, CHI de Creteil and Inserm U676, Hospital Robert Debre, Paris, France: H. Adle-Biassette; Czech; Department of Neurology and Pathology and Molecular Medicine, Charles University, 2nd Faculty of Medicine, Motol University Hospital, Prague, Czech Republic: P. Krsek, J. Zamecnik; Department of Neuropathology, John Radcliffe Hospital, Oxford, UK: C. Kennard; Department of Anatomic Pathology Sciences, Università Sapienza, Rome, Italy: M. Antonelli, F. Giangaspero; Institute of Neuropathology, Westfälische Wilhelms – Universität Münster, Münster, Germany: W. Paulus, M. Hasselblatt; Department of Neuropathology, University Hospital Erlangen, Erlangen, Germany: R. Coras, I. Blümcke; Bethel Epilepsy Centre, Bielefeld, Germany: T. Polster, C.G. Bien; Laboratory of Neuropathology, Department of Neurology, Hospital de Santa Maria [CHLN], Lisbon, Portugal: J. Pimentel; Department of Pathology, Faculty of Medicine, Hacettepe University, Ankara, Turkey: F. Söylemezoğlu). In this regard we would like to acknowledge all personnel involved in sending us brain tissue. Furthermore, the authors would like to thank Dr Mark Nellist (Department of Clinical Genetics, Erasmus Medical Centre, Rotterdam, The Netherlands) and Dr David J. Kwiatkowski, MD, PhD (Division of Experimental Medicine and Medical Oncology, Brigham and Women's Hospital, Boston) for performing TSC1/TSC2 mutation analysis. We acknowledge the HIS Mouse Facility of the Amsterdam UMC and the Bloemenhove Clinic (Heemstede, The Netherlands) for providing fetal tissues.

REFERENCES

1. Curatolo P, Bombardieri R, Jozwiak S. Tuberous sclerosis. Lancet 2008; 372:657–68
2. DiMario FJ. Jr Brain abnormalities in tuberous sclerosis complex. J Child Neurol 2004;19:650–7
3. European Chromosome 16 Tuberous Sclerosis C. Identification and characterization of the tuberous sclerosis gene on chromosome 16. Cell 1993; 75:1305–15
4. van Slegtenhorst M, de Hoogt R, Hermans C, et al. Identification of the tuberous sclerosis gene TSC1 on chromosome 9q34. Science 1997;277: 805–8
5. Kwiatkowski DJ. Rhebbing up mTOR: New insights on TSC1 and TSC2, and the pathogenesis of tuberous sclerosis. Cancer Biol Ther 2003;2: 471–6
6. Chan JA, Zhang H, Roberts PS, et al. Pathogenesis of tuberous sclerosis subependymal giant cell astrocytomas: Biallelic inactivation of TSC1 or TSC2 leads to mTOR activation. J Neuropathol Exp Neurol 2004;63: 1236–42
7. Inoki K, Li Y, Zhu T, et al. TSC2 is phosphorylated and inhibited by Akt and suppresses mTOR signalling. Nat Cell Biol 2002;4:648–57
8. Laplante M, Sabatini DM. Regulation of mTORC1 and its impact on gene expression at a glance. J Cell Sci 2013;126:1713–9
9. Aronica E, Becker AJ, Spreafico R. Malformations of cortical development. Brain Pathol 2012;22:380–401
10. Aronica E, Crino PB. Epilepsy related to developmental tumors and malformations of cortical development. Neurotherapeutics 2014;11:251–68
11. Mizuguchi M, Takashima S. Neuropathology of tuberous sclerosis. Brain Dev 2001;23:508–15
12. Adriaensen ME, Schaefer-Prokop CM, Stijnen T, et al. Prevalence of subependymal giant cell tumors in patients with tuberous sclerosis and a review of the literature. Eur J Neurol 2009;16:691–6
13. Kingswood JC, d'Augeres GB, Belousova E, et al. TuberOus SClerosis registry to increase disease Awareness (TOSCA)—Baseline data on 2093 patients. Orphanet J Rare Dis 2017;12:2
14. Kothare SV, Singh K, Chalifoux JR, et al. Severity of manifestations in tuberous sclerosis complex in relation to genotype. Epilepsia 2014;55: 1025–9

15. Goh S, Butler W, Thiele EA. Subependymal giant cell tumors in tuberous sclerosis complex. Neurology 2004;63:1457–61
16. Cuccia V, Zuccaro G, Sosa F, et al. Subependymal giant cell astrocytoma in children with tuberous sclerosis. Childs Nerv Syst 2003;19:232–43
17. Amin S, Carter M, Edwards RJ, et al. The outcome of surgical management of subependymal giant cell astrocytoma in tuberous sclerosis complex. Eur J Paediatr Neurol 2013;17:36–44
18. Curatolo P, Moavero R, de Vries PJ. Neurological and neuropsychiatric aspects of tuberous sclerosis complex. Lancet Neurol 2015;14:733–45
19. Bonnin JM, Rubinstein LJ, Papasozomenos SC, et al. Subependymal giant cell astrocytoma. Significance and possible cytogenetic implications of an immunohistochemical study. Acta Neuropathol 1984;62:185–93
20. Buccoliero AM, Franchi A, Castiglione F, et al. Subependymal giant cell astrocytoma (SEGA): Is it an astrocytoma? Morphological, immunohistochemical and ultrastructural study. Neuropathology 2009;29:25–30
21. Fujiwara S, Takaki T, Hikita T, et al. Subependymal giant-cell astrocytoma associated with tuberous sclerosis. Do subependymal nodules grow? Child's Nerv Syst 1989;5:43–4
22. Morimoto K, Mogami H. Sequential CT study of subependymal giant-cell astrocytoma associated with tuberous sclerosis. Case report. J Neurosurg 1986;65:874–7
23. Bongaarts A, Giannikou K, Reinten RJ, et al. Subependymal giant cell astrocytomas in Tuberous Sclerosis Complex have consistent TSC1/TSC2 biallelic inactivation, and no BRAF mutations. Oncotarget 2017;8:95516–29
24. Martin KR, Zhou W, Bowman MJ, et al. The genomic landscape of tuberous sclerosis complex. Nat Commun 2017;8:15816
25. Tyburczy ME, Kotulska K, Pokarowski P, et al. Novel proteins regulated by mTOR in subependymal giant cell astrocytomas of patients with tuberous sclerosis complex and new therapeutic implications. Am J Pathol 2010;176:1878–90
26. Bongaarts A, van Scheppingen J, Korotkov A, et al. The coding and non-coding transcriptional landscape of subependymal giant cell astrocytomas. Brain 2020;143:131–49
27. Boer K, Crino PB, Gorter JA, et al. Gene expression analysis of tuberous sclerosis complex cortical tubers reveals increased expression of adhesion and inflammatory factors. Brain Pathol 2009;20:704–19
28. Broekaart DWM, van Scheppingen J, Anink JJ, et al. Increased matrix metalloproteinases expression in tuberous sclerosis complex: Modulation by microRNA 146a and 147b in vitro. Neuropathol Appl Neurobiol 2020;46:142–59
29. Mills JD, Iyer AM, van Scheppingen J, et al. Coding and small non-coding transcriptional landscape of tuberous sclerosis complex cortical tubers: Implications for pathophysiology and treatment. Sci Rep 2017;7:8089
30. Rivera S, Khrestchatisky M, Kaczmarek L, et al. Metzincin proteases and their inhibitors: Foes or friends in nervous system physiology? J Neurosci 2010;30:15337–57
31. Nagase H, Visse R, Murphy G. Structure and function of matrix metalloproteinases and TIMPs. Cardiovasc Res 2006;69:562–73
32. Sternlicht MD, Werb Z. How matrix metalloproteinases regulate cell behavior. Annu Rev Cell Dev Biol 2001;17:463–516
33. Shi YB, Fu L, Hasebe T, et al. Regulation of extracellular matrix remodeling and cell fate determination by matrix metalloproteinase stromelysin-3 during thyroid hormone-dependent post-embryonic development. Pharmacol Ther 2007;116:391–400
34. Wang L, Zhang ZG, Zhang RL, et al. Matrix metalloproteinase 2 (MMP2) and MMP9 secreted by erythropoietin-activated endothelial cells promote neural progenitor cell migration. J Neurosci 2006;26:5996–6003
35. Rundhaug JE. Matrix metalloproteinases and angiogenesis. J Cell Mol Med 2005;9:267–85
36. Rosenberg GA, Yang Y. Vasogenic edema due to tight junction disruption by matrix metalloproteinases in cerebral ischemia. Neurosurg Focus 2007;22:1–9
37. Van Lint P, Libert C. Chemokine and cytokine processing by matrix metalloproteinases and its effect on leukocyte migration and inflammation. J Leukoc Biol 2007;82:1375–81
38. Nakamura H, Suenaga N, Taniwaki K, et al. Constitutive and induced CD44 shedding by ADAM-like proteases and membrane-type 1 matrix metalloproteinase. Cancer Res 2004;64:876–82
39. Lee KY, Kim YJ, Yoo H, et al. Human brain endothelial cell-derived COX-2 facilitates extravasation of breast cancer cells across the blood-brain barrier. Anticancer Res 2011;31:4307–13
40. Belien AT, Paganetti PA, Schwab ME. Membrane-type 1 matrix metalloprotease (MT1-MMP) enables invasive migration of glioma cells in central nervous system white matter. J Cell Biol 1999;144:373–84
41. Vandenbroucke RE, Libert C. Is there new hope for therapeutic matrix metalloproteinase inhibition? Nat Rev Drug Discov 2014;13:904–27
42. Friedman RC, Farh KK, Burge CB, et al. Most mammalian mRNAs are conserved targets of microRNAs. Genome Res 2008;19:92–105
43. Bartel DP. MicroRNAs: Genomics, biogenesis, mechanism, and function. Cell 2004;116:281–97
44. Ha TY. MicroRNAs in human diseases: From cancer to cardiovascular disease. Immune Netw 2011;11:135–54
45. Cao DD, Li L, Chan WY. MicroRNAs: Key regulators in the central nervous system and their implication in neurological diseases. Int J Mol Sci 2016;17:842
46. Reschke CR, Henshall DC. MicroRNA and epilepsy. Adv Exp Med Biol 2015;888:41–70
47. van Scheppingen J, Iyer AM, Prabowo AS, et al. Expression of microRNAs miR21, miR146a, and miR155 in tuberous sclerosis complex cortical tubers and their regulation in human astrocytes and SEGA-derived cell cultures. Glia 2016;64:1066–82
48. van Scheppingen J, Mills JD, Zimmer TS, et al. miR147b: A novel key regulator of interleukin 1 beta-mediated inflammation in human astrocytes. Glia 2018;66:1082–97
49. Qin CZ, Lv QL, Yang YT, et al. Downregulation of microRNA-320d predicts poor overall survival and promotes the growth and invasive abilities in glioma. Chem Biol Drug Des 2017;89:806–14
50. Xia H, Qi Y, Ng SS, et al. MicroRNA-146b inhibits glioma cell migration and invasion by targeting MMPs. Brain Res 2009;1269:158–65
51. Louis DN, Perry A, Reifenberger G, et al. The 2016 World Health Organization classification of tumors of the central nervous system: A summary. Acta Neuropathol 2016;131:803–20
52. Northrup H, Krueger DA, Northrup H, et al. International Tuberous Sclerosis Complex Consensus G. Tuberous sclerosis complex diagnostic criteria update: Recommendations of the 2012 International Tuberous Sclerosis Complex Consensus Conference. Pediatr Neurol 2013;49:243–54
53. Kim D, Pertea G, Trapnell C, et al. TopHat2: Accurate alignment of transcriptomes in the presence of insertions, deletions and gene fusions. Genome Biol 2013;14:R36
54. Liao Y, Smyth GK, Shi W. featureCounts: An efficient general purpose program for assigning sequence reads to genomic features. Bioinformatics 2014;30:923–30
55. Love MI, Huber W, Anders S. Moderated estimation of fold change and dispersion for RNA-Seq data with DESeq2. Genome Biol 2014;15:550
56. Croft D, O'Kelly G, Wu G, et al. Reactome: A database of reactions, pathways and biological processes. Nucleic Acids Res 2011;39:D691–7
57. Fabregat A, Jupe S, Matthews L, et al. The Reactome pathway knowledgebase. Nucleic Acids Res 2018;46:D649–55
58. Dweep H, Gretz N, Sticht C. miRWalk database for miRNA-target interactions. Methods Mol Biol 2014;1182:289–305
59. Dweep H, Sticht C, Pandey P, et al. miRWalk—Database: Prediction of possible miRNA binding sites by "walking" the genes of three genomes. J Biomed Inform 2011;44:839–47
60. Bongaarts A, Prabowo AS, Arena A, et al. MicroRNA519d and microRNA4758 can identify gangliogliomas from dysembryoplastic neuroepithelial tumours and astrocytomas. Oncotarget 2018;9:28103–15
61. Ruijter JM, Ramakers C, Hoogaars WM, et al. Amplification efficiency: Linking baseline and bias in the analysis of quantitative PCR data. Nucleic Acids Res 2009;37:e45
62. Boer K, Jansen F, Nellist M, et al. Inflammatory processes in cortical tubers and subependymal giant cell tumors of tuberous sclerosis complex. Epilepsy Res 2008;78:7–21
63. Prabowo AS, Anink JJ, Lammens M, et al. Fetal brain lesions in tuberous sclerosis complex: TORC1 activation and inflammation. Brain Pathol 2013;23:45–59
64. Zhang B, Zou J, Rensing NR, et al. Inflammatory mechanisms contribute to the neurological manifestations of tuberous sclerosis complex. Neurobiol Dis 2015;80:70–9

65. van Vliet EA, Aronica E, Gorter JA. Blood-brain barrier dysfunction, seizures and epilepsy. Semin Cell Dev Biol 2015;38:26–34
66. Van den Steen PE, Proost P, Wuyts A, et al. Neutrophil gelatinase B potentiates interleukin-8 tenfold by aminoterminal processing, whereas it degrades CTAP-III, PF-4, and GRO-alpha and leaves RANTES and MCP-2 intact. Blood 2000;96:2673–81
67. Schonbeck U, Mach F, Libby P. Generation of biologically active IL-1 beta by matrix metalloproteinases: A novel caspase-1-independent pathway of IL-1 beta processing. J Immunol 1998;161:3340–6
68. Mohan MJ, Seaton T, Mitchell J, et al. The tumor necrosis factor-alpha converting enzyme (TACE): A unique metalloproteinase with highly defined substrate selectivity. Biochemistry 2002;41:9462–9
69. Gidday JM, Gasche YG, Copin JC, et al. Leukocyte-derived matrix metalloproteinase-9 mediates blood-brain barrier breakdown and is proinflammatory after transient focal cerebral ischemia. Am J Physiol Heart Circ Physiol 2005;289:H558–68
70. Justicia C, Panes J, Sole S, et al. Neutrophil infiltration increases matrix metalloproteinase-9 in the ischemic brain after occlusion/reperfusion of the middle cerebral artery in rats. J Cereb Blood Flow Metab 2003;23: 1430–40
71. Ramachandran RK, Sorensen MD, Aaberg-Jessen C, et al. Expression and prognostic impact of matrix metalloproteinase-2 (MMP-2) in astrocytomas. PLoS One 2017;12:e0172234
72. Wang L, Yuan J, Tu Y, et al. Co-expression of MMP-14 and MMP-19 predicts poor survival in human glioma. Clin Transl Oncol 2013;15: 139–45
73. Thorns V, Walter GF, Thorns C. Expression of MMP-2, MMP-7, MMP-9, MMP-10 and MMP-11 in human astrocytic and oligodendroglial gliomas. Anticancer Res 2003;23:3937–44
74. Stojic J, Hagemann C, Haas S, et al. Expression of matrix metalloproteinases MMP-1, MMP-11 and MMP-19 is correlated with the WHO-grading of human malignant gliomas. Neurosci Res 2008;60: 40–9
75. Kachra Z, Beaulieu E, Delbecchi L, et al. Expression of matrix metalloproteinases and their inhibitors in human brain tumors. Clin Exp Metastasis 1999;17:555–66
76. Atkinson SJ, Crabbe T, Cowell S, et al. Intermolecular autolytic cleavage can contribute to the activation of progelatinase A by cell membranes. J Biol Chem 1995;270:30479–85
77. Itoh Y, Takamura A, Ito N, et al. Homophilic complex formation of MT1-MMP facilitates proMMP-2 activation on the cell surface and promotes tumor cell invasion. EMBO J 2001;20:4782–93
78. Lettau I, Hattermann K, Held-Feindt J, et al. Matrix metalloproteinase-19 is highly expressed in astroglial tumors and promotes invasion of glioma cells. J Neuropathol Exp Neurol 2010;69:215–23
79. Korotkov A, Broekaart DWM, van Scheppingen J, et al. Increased expression of matrix metalloproteinase 3 can be attenuated by inhibition of microRNA-155 in cultured human astrocytes. J Neuroinflamm 2018; 15:211